A Tethered Agonist within the Ectodomain Activates the Adhesion G Protein-coupled Receptors GPR126 and GPR133

Ines Liebscher[1;4]*†, Julia Schön[1]†, Sarah C. Petersen[2], Liane Fischer[1], Nina Auerbach[1,2], Lilian Marie Demberg[1], Amit Mogha[2], Maxi Cöster[1], Kay-Uwe Simon[1], Sven Rothemund[3], Kelly R. Monk[2] & Torsten Schöneberg[1]*

[1]Institute of Biochemistry, Medical Faculty, University of Leipzig, 04103 Leipzig, Germany
[2]Department of Developmental Biology, Washington University School of Medicine, St. Louis, MO 63110 USA
[3]Core Unit Peptide Technologies, Medical Faculty, University of Leipzig, 04103 Leipzig, Germany
[4]Novo Nordisk Center for Basic Metabolic Research, Department of Biomedical Sciences, University of Copenhagen, DK-2200 Copenhagen, Denmark

*Correspondence to: T.S. (schoberg@medizin.uni-leipzig.de) or I.L. (liebscher@medizin.uni-leipzig.de).
†contributed equally to this work

Supplementary Methods

Generation of wildtype and mutant adhesion GPCR constructs - Full-length human aGPCR sequences were amplified from a human monocyte cDNA library and directly cloned into the mammalian expression vector pcDps. Wild-type (wt) and mutant zebrafish Gpr126 were amplified from cDNA generated from a pool of 3 dpf larvae of the appropriate genotypes except for the *stl215* ΔGly^{831}-Ile^{832}, which was generated by PCR-based site-directed mutagenesis. For detection purposes and to increase cell surface expression, a hemagglutinin (HA) epitope was inserted directly downstream of the predicted signal peptide (SignalP 4.1 server; http://www.cbs.dtu.dk/services/SignalP) of all aGPCRs used in this study by a PCR-based site-directed mutagenesis and fragment replacement strategy. Further, a FLAG epitope was introduced at the very C terminus of all constructs.

Detailed structure function analyses were performed with GPR126 and GPR133. Changes in their architecture, chimeras and point mutations were generated by PCR and homologous recombination in *E. coli* from Invitrogen (Darmstadt, Germany). The sequence of all wt aGPCRs and derived constructs were verified by sequencing. A detailed description of all constructs is given in suppl. Table S1.

Detection of endogenously expressed Gpr126 with real time PCR - Total RNA was extracted from COS-7 cells using TRIzol reagent (Invitrogen) according to the manufacturer's instructions. Total RNA was further purified with RNeasy kits (Qiagen, Hilden, Germany) according to the RNA clean-up protocol. For real-time PCR analysis (rtPCR), total RNA was reversely transcribed (Superscript II, Invitrogen) with oligo(dT) primer. Primer sequences that align with primate beta actin (s: 5'-cgagaagatgacccagatcatg-3'; as: 5'-ggactccatgcccaggaag-3') and conserved sequences of Gpr126 (s: 5'-atcagagttgccgtgtcctt-3'; as: 5'-ggaaccacagcttaggttgc-3') were used to amplify specific PCR bands.

Functional assays - aGPCRs were heterologously expressed in COS-7 cells grown in Dulbecco's minimum essential medium (DMEM) supplemented with 10% fetal bovine serum, 100 units/ml penicillin and 100 µg/ml streptomycin at 37° C and 5% CO_2 in a humidified atmosphere. For assays, cells were split into 48-well plates (3×10^4 cells/well) and transfected with Lipofectamine™ 2000 (Invitrogen, Paisley, UK) according to the manufacturer's protocol. We used 500 ng when measuring basal activity and 100 ng when measuring response to peptides of plasmid DNA/well. Empty vector stimulated with 10 µM of forskolin served as positive control for cAMP accumulation. 48 h after transfection, cells were incubated with 3-isobutyl-methyl-xanthine (1 mM)-containing medium, lysed in LI buffer (PerkinElmer Life Sciences, Monza, Italy) and kept frozen at −20° C until measurement. To measure cAMP concentration, the Alpha Screen cAMP assay kit (PerkinElmer Life Sciences) was used according to the manufacturer's protocol. The accumulation was measured in 384-well white OptiPlate microplates (PerkinElmer Life Sciences) with the Fusion AlphaScreen multilabel reader (PerkinElmer Life Sciences). For siRNA experiments, 5 pmol/well h*GPR126* siRNA (sc-95410; Santa Cruz Biotechnology, Heidelberg, Germany) and control siRNA (sc-37007; Santa Cruz Biotechnology) were co-transfected into COS-7 cells with plasmids encoding the pcDps or human GPR126. Assay data was analyzed using GraphPad Prism version 6.0 for Windows (GraphPad Software, San Diego, CA).

To estimate cell surface expression of receptors carrying an N-terminal HA tag, an indirect cellular enzyme-linked immunosorbent assay (ELISA) was used (Schoneberg et al., 1998). To

assess the amounts of full-length HA/FLAG double-tagged constructs in cells, a sandwich ELISA was performed as described (Rompler et al., 2006).

Peptide synthesis - Solid phase peptide synthesis of the peptides was performed on an automated peptide synthesizer MultiPep from Intavis AG (Köln, Germany) using standard Fmoc-chemistry. The final side chain deprotection and cleavage from the solid support employed a mixture of TFA, water and thioanisole (95:2.5:2.5, vol %) for the peptides. The peptides were purified to >95 % purity using preparative RP-HPLC (Shimadzu LC-8, Duisburg, Germany) equipped with a PLRP-S column (300x25mm, Agilent, Waldbronn, Germany). For both analytical and preparative use, the mobile phases were water (A) and acetonitrile (B), respectively, each containing 0.1 % TFA. Samples were eluted with a linear gradient from 5% B to 90% B in 30 min for analytical runs and in 90 min for preparative runs.

Finally, all peptides were characterized by analytical HPLC (Agilent 1100) and MALDI-MS (Bruker Microflex LT, Bremen, Germany), which gave the expected $[M^{+}H]^{+}$ mass peaks.

Epic measurements - To measure label-free receptor activation, a dynamic mass redistribution (DMR) assay (Corning Epic Biosensor Measurements; Corning Life Sciences, Lowell, MA) with COS-7 cells endogenously expressing GPR126 was performed as described previously (Schroder et al., 2010). Briefly, cells were seeded into fibronectin-coated Epic 384–well microplates at a density of 6,000 cells per well and cultured for 24 h to reach confluent monolayers. After 2 h of equilibration, the cells were then stimulated and DMR was recorded for 3,000 s.

Western Blot Analysis - Conditioned medium was collected from cells 48 h post transfection, pelleted by centrifugation and protease inhibitor (complete Protease Inhibitor Cocktail Tablets, Roche) was added. Protein was subject to electrophoresis in a 10 % sodium dodecyl sulfate-polyacrylamide gel electrophoresis (SDS-PAGE) gel and transferred to a polyvinylidene difluoride membranes. Blots were then probed with a POD-conjugated anti-HA antibody (Roche) 1:1,000, overnight at 4°C. Western blots were developed by an enhanced chemiluminescence (ECL) detection system (Thermo Scientific). For detection of actin as loading control, membranes were stripped in Stripping buffer (1% SDS, 0.1 M Tris pH 6.8, 0.175% β-mercaptoethanol) for 30 min at 50°C, blocked and probed with rabbit anti-β actin (Sigma Aldrich) 1:1,000, and then incubated with horseradish-peroxidase–conjugated goat anti-rabbit (Sigma Aldrich) 1:3,000 and developed as described above.

Zebrafish maintenance and mutant strains - Zebrafish were maintained in the Washington University Zebrafish Consortium facility (http://zebrafish.wustl.edu/husbandry.htm) and all experiments were performed in compliance with Washington University's institutional animal protocols. Collected embryos were reared at 28.5° C and staged in hours post-fertilization (hpf) or days post-fertilization (dpf) following standard protocols. The strains used in the experiments were WT (AB*), *gpr126*^{stl215} (genotyping/generation described below), *gpr126*^{st49} and *gpr126*^{st63} (Monk et al 2009)**.** Genotyping of *st63* and *st49* was performed as previously described (Monk et al 2009).

Generation of *gpr126*^{stl215} mutants via TALENs - The *stl215* allele was generated by Transcription-Activator-Like-Effector-Nuclease (TALEN) technology. The TALEN was designed with the TALEN Targeter tool (https://tale-nt.cac.cornell.edu/) and cloned by the Transgenic Vector Core at Washington University in St. Louis School of Medicine. Left repeat variable diresidue (RVD) sequence: HD NG NN HD NG NG NN NG NN NG NI NI NG HD NI HD HD NG HD NI. Right RVD sequence: HD HD HD NI HD NI NI NI NG HD NG HD NI HD HD NI NG NG NI. The assembled TALEN arms in pCS2+ vector were separately transcribed

with the mMESSAGE mMACHINE® SP6 ULTRA kit (Ambion, Grand Island, NY). A total of 50 pg combined TALEN mRNA (25 pg of left and 25 pg of right arm) was microinjected in WT AB* embryos at the one-cell stage. Injected F0s were raised and outcrossed to WT AB*; resulting F1s were screened for stable germline-transmitted lesions. Screening was performed with 24 hpf gDNA using the genotyping assay described below, followed by Sanger sequencing of PCR products cloned into pCRII via TOPO®TA Cloning® kit (Invitrogen, Grand Island, NY). Zebrafish carrying the *stl215* allele were intercrossed and their offspring analyzed (F2 generation). Wild-type siblings were used for controls in analysis.

***stl215* genotyping** - Starting from genomic DNA, a 397 bp long region containing the TALEN-targeted enzyme site was amplified with following primers: F: 5'-CCGAATCCTCAGTGTGTGTT-3' and R: 5'-GTCAATACTTAGGGGCTTCGC-3'. The wt PCR product has an intact BtsCI binding site and is therefore cleaved by the enzyme in two fragments of 239 bp and 158bp. The Δ6 deletion in *gpr126*^{stl215} disrupts the BtsCI site and results in the retention of the 397 bp product.

Whole mount *in situ* hybridization (WISH) and analysis - Larvae from heterozygous parents were raised in egg water + 0.003% PTU to prevent pigmentation and fixed with 4% paraformaldehyde at 4 or 5 dpf. WISH was performed according to standard protocols (Thisse et al., 1994). We used an established *mbp* riboprobe (Lyons et al., 2005) to visualize *mbp* expression in the central and peripheral nervous systems. For all experiments, *mbp* expression was scored with observer blind to genotype and treatment. For *stl215* phenotypic analyses, two biological replicates were performed.

Zebrafish transmission electron microscopy (TEM) and analysis - Larvae from heterozygous matings were processed for TEM as described (Czopka and Lyons, 2011) using a Pelco BioWave Pro with Steady Temp Plus water recirculation system (Ted Pella Inc., Redding, CA). Ultrathin (70 nm) sections were mounted on mesh copper grids and stained with saturated uranyl acetate and Sato's lead stain. Samples were viewed on a Jeol JEM-1400 (Jeol USA, Peabody, MA) and micrographs were obtained with an AMT V601 digital camera (Advanced Microscopy Techniques, Corp., Woburn, MA). Average number of total, sorted, and myelinated axons was scored in n=6 nerves from n=4 larvae each of wt and *gpr126*^{stl215} and significance was determined using Student's t-test.

Zebrafish peptide treatment and analysis - Larvae from heterozygous matings were treated from 50-55 hours post-fertilization stages (Kimmel et al., 1995) in 5 mL egg water supplemented with 100 μM p16 or an equivalent volume of DMSO. Samples for WISH were also simultaneously treated with 0.003% PTU. As a positive control, siblings were treated with 50 μM forskolin (not shown). Following treatment, larvae were washed twice with fresh egg water and raised for three more days at 28.5° C to 5 dpf. Samples were then processed for WISH or TEM as described above. Three technical and four biological replicates were performed for *st63* and one technical replicate was performed (parallel to *st63*) for *st49*. Statistical analysis was performed by grouping "none" and "weak" classes (*i.e.*, typical *st63* phenotype) into a single group (n=21 for DMSO, n=18 for p16) and comparing against grouped "some" and "strong" classes (atypical for *st63*; n=0 for DMSO, n=14 for p16) with Fisher's Exact Test.

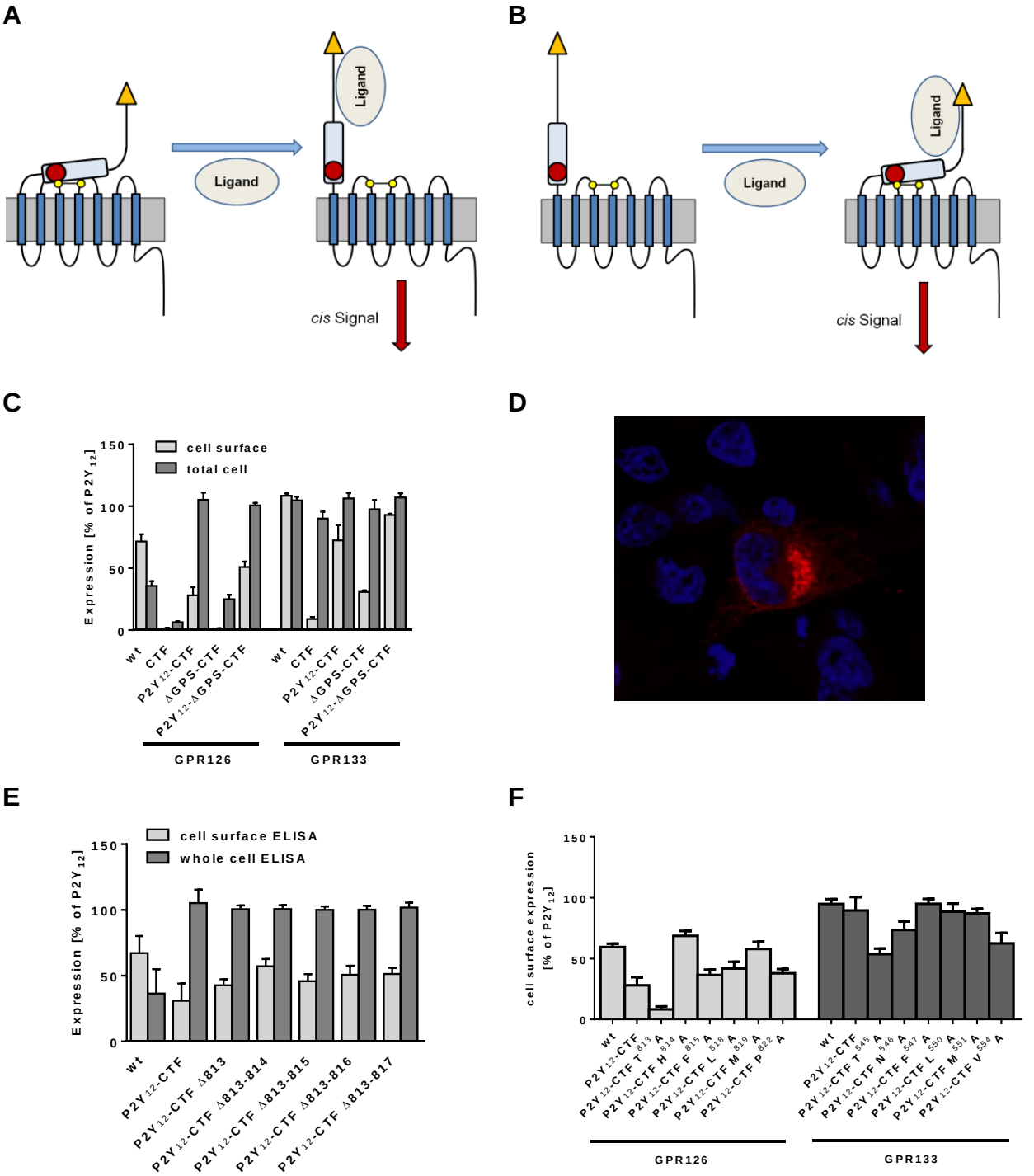
A
Ligand
Ligand
cis Signal
B
Ligand
Ligand
cis Signal
C
cell surface
total cell
Expression [% of P2Y12]
150
100
50
0
wt
CTF
P2Y12-CTF
ΔGPS-CTF
P2Y12-ΔGPS-CTF
wt
CTF
P2Y12-CTF
ΔGPS-CTF
P2Y12-ΔGPS-CTF
GPR126
GPR133
D
E
cell surface ELISA
whole cell ELISA
Expression [% of P2Y12]
150
100
50
0
wt
P2Y12-CTF
P2Y12-CTF Δ813
P2Y12-CTF Δ813-814
P2Y12-CTF Δ813-815
P2Y12-CTF Δ813-816
P2Y12-CTF Δ813-817
F
cell surface expression [% of P2Y12]
150
100
50
0
wt
P2Y12-CTF
P2Y12-CTF T813A
P2Y12-CTF H814A
P2Y12-CTF F815A
P2Y12-CTF L818A
P2Y12-CTF M819A
P2Y12-CTF P822A
wt
P2Y12-CTF
P2Y12-CTF T545A
P2Y12-CTF N546A
P2Y12-CTF F547A
P2Y12-CTF L550A
P2Y12-CTF M551A
P2Y12-CTF V554A
GPR126
GPR133

Suppl. Figure S1. Models of aGPCR activation and expression analysis of wt and mutant GPR126 and GPR133 constructs, Related to Figure 1

Two models of aGPCR activation have been proposed: (**A**) the N terminus contains a tethered inverse agonist that inhibits 7TM signaling until ligand binding at the ECD or artificial removal of the ECD. (**B**) Binding of a ligand at the ECD or removal of parts of the ECD changes its conformation and exposes a tethered agonist. (**C**) COS-7 cells were transfected with wt and mutant GPR126 and GPR133 constructs. For expression studies, cell surface and sandwich ELISA were used to measure cell surface and total cellular expression levels, respectively. Specific optical density (OD) readings are given as percentage of the human $P2Y_{12}$. (**D**) COS-7 cells were transfected with CTF(GPR126), and permeabilized cells were incubated with a monoclonal antibody directed against the C-terminal FLAG-tag. A TRITC-conjugated antibody was used to detect the monoclonal antibody. Nuclei are stained with DAPI. Imaging was performed using a confocal microscope (Zeiss LSM 510). A representative picture shows membrane localization of CTF(GPR126) (red). (**E**) Sequential aa were deleted in $P2Y_{12}$-CTF(GPR126) and expression levels in whole cells and at the cell surface were determined through ELISA studies as described under *Experimental Procedures*. Specific optical density (OD) readings are given as percentage of the human $P2Y_{12}$. (**F**) Single positions within the C-terminal GPS sequence were mutated in GPR126 and GPR133 to alanine, and cell surface expression was determined through ELISA measurement. Specific optical density (OD) readings are given as percentage of the human $P2Y_{12}$. For (C), (E) and (F): Specific optical density (OD) readings (OD value of double HA/FLAG-tagged aGPCR constructs minus OD value of mock-transfected cells) are given as percentage of the human $P2Y_{12}$ receptor, which served as positive control. For the cell surface ELISA, the non-specific OD value (pcDps) was 0.03 ± 0.03 (set 0%) and the OD value of $P2Y_{12}$ was 1.30 ± 0.24 (set 100%). OD readings of 0.08 ± 0.04 (set 0%) and 2.22 ± 0.73 (set 100%) were found in sandwich ELISA (total expression) for the empty vector negative (pcDps) and positive control ($P2Y_{12}$). Data are given as means ± SEM for at least three independent experiments each performed in triplicates.

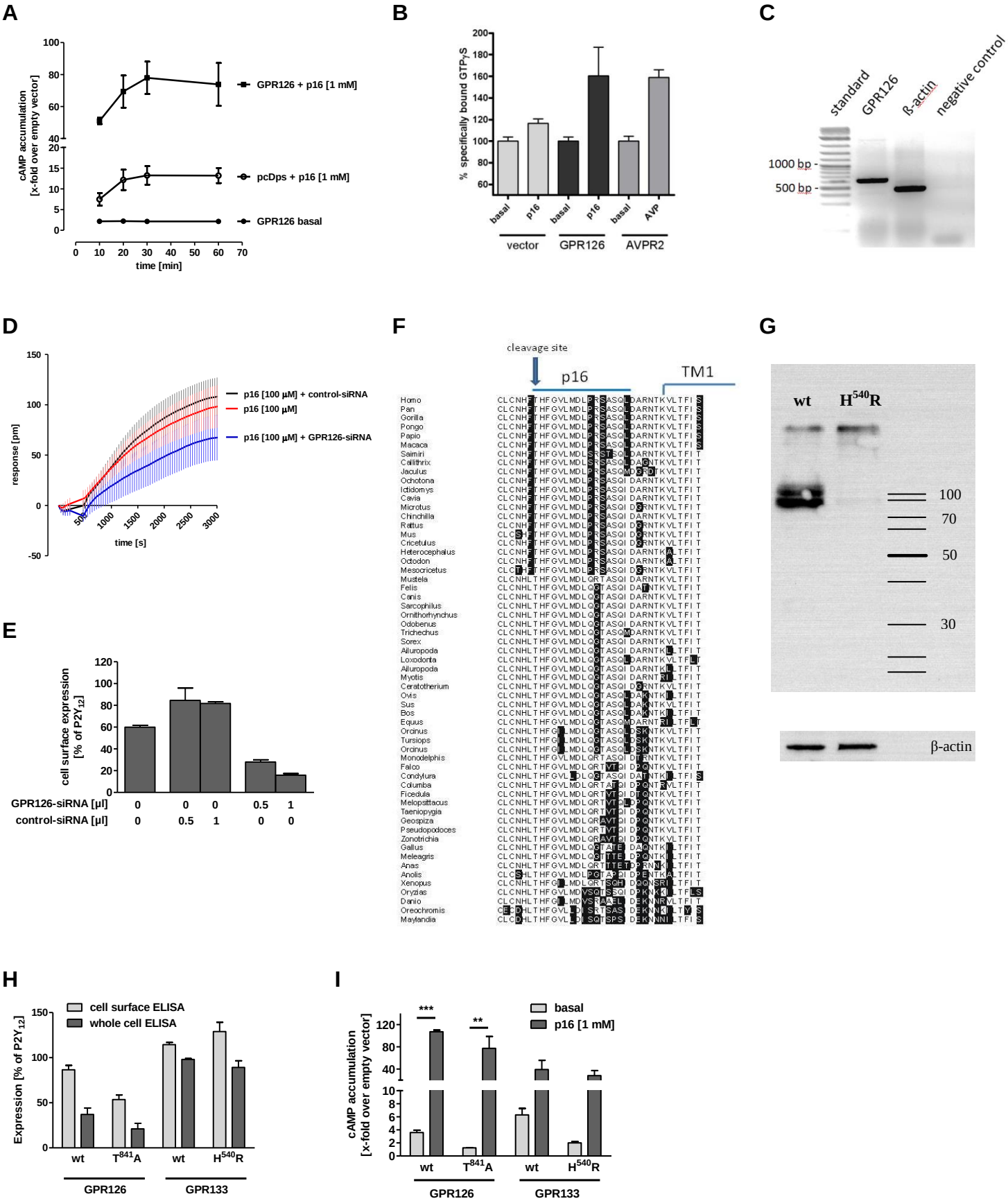
A
cAMP accumulation [x-fold over empty vector]
time [min]
GPR126 + p16 [1 mM]
pcDps + p16 [1 mM]
GPR126 basal
B
% specifically bound GTPγS
basal
p16
basal
p16
basal
AVP
vector
GPR126
AVPR2
C
standard
GPR126
β-actin
negative control
1000 bp
500 bp
D
response [pm]
time [s]
p16 [100 µM] + control-siRNA
p16 [100 µM]
p16 [100 µM] + GPR126-siRNA
E
cell surface expression [% of P2Y12]
GPR126-siRNA [µl]
control-siRNA [µl]
F
cleavage site
p16
TM1
G
wt
H540R
100
70
50
30
β-actin
H
cell surface ELISA
whole cell ELISA
Expression [% of P2Y12]
wt
T841A
wt
H540R
GPR126
GPR133
I
basal
p16 [1 mM]
cAMP accumulation [x-fold over empty vector]
wt
T841A
wt
H540R
GPR126
GPR133

Suppl. Figure S2. Specification of *Stachel* peptide mediated activation of GPR126 and GPR133, Related to Figure 2

(**A**) COS-7 cells were transiently transfected with GPR126 and empty vector plasmid and tested for basal and stimulated cAMP accumulation at several time points shown as x-fold over empty vector. While basal receptor activity remains constant, p16-derived activity increases starting at 10 minutes until it reaches a stable maximum after 30 minutes. Basal cAMP levels were: 10 minutes: 6.01 ± 2.93 nM; 20 minutes: 7.19 ± 2.30 nM; 30 minutes: 7.31 ± 2.66 nM; 60 minutes: 7.43 ± 2.77 nM. The mean ± SEM of three independent experiments performed in triplicate is shown. (**B**) Membranes prepared from empty vector- and GPR126-transfected cells were used to perform [^{35}S]GTPγS binding assays as described in (Gupte et al., 2012). Incubation was performed for 1 hour in the presence of 0.5 nM [^{35}S]GTPγS, 0.1 nM GDP and 1 mM p16. For control purposes, COS-7 cells were transfected with the G_s-coupled V2 vasopressin receptor and stimulated with 100 nM Arg-vasopressin (Boselt et al., 2009). Non-specific [^{35}S]GTPγS binding was determined in the presence of non-radioactive GTPγS (100 nM). Data are presented as mean ± SEM of two independent experiments, each carried out in triplicates. (**C**) *GPR126* is endogenously expressed in COS-7 cells causing residual activation by p16 of non-transfected cells. Using primers that align to conserved regions of *GPR126*, transcripts were amplified from COS-7 cell cDNA. Reactions lacking cDNA and containing β-actin specific primers served as negative and positive controls, respectively. (**D**) For label-free measurements of receptor activation, a dynamic mass redistribution assay (Epic Biosensor Measurements) with COS-7 cells endogenously expressing GPR126 was performed. GPR126-specific siRNA abolished p16-induced responses. Data are presented as mean ± SEM of at least three independent experiments, each carried out in quadruplicates. (**E**) A cell surface ELISA was used to evaluate the efficiency of GPR126 siRNA knockdown. COS-7 cells were transiently transfected with GPR126 plasmid alone or co-transfected with either control-siRNA or siRNA targeted against GPR126. Specific optical density (OD) readings are given as percentage of the human $P2Y_{12}$. The non-specific OD value (pcDps) was 0.05 ± 0.03 (set 0%) and the OD value of $P2Y_{12}$ was 2.23 ± 0.06 (set 100%). Data are presented as mean ± SD of one representative experiment, carried out in triplicates. (**F**) Alignment of various vertebrate species revealed presence of conserved GPR126 p16 sequence (downstream the GPR126 cleavage site) in all vertebrate classes. Positions that differ from the majority are boxed in black. The tethered agonistic peptide (p16), cleavage site and the beginning of transmembrane helix 1 (TM1) are marked. (**G**) Because the importance of cleavage for aGPCR expression and activity has been controversially discussed (Liebscher et al., 2013), we tested two cleavage-deficient mutants. Cleavage deficiency has been reported for GPR126T^{841}A (Moriguchi et al., 2004). The lack of autoproteolytic cleavage in GPR133H^{540}R is demonstrated by western blot analysis. wt GPR133 shows a double band at ~100 kDa, which is absent in GPR133H^{540}R, while β-actin controls display equal amounts of protein in both lanes. Human GPR126T^{841}A and mouse GPR133H^{540}R were analyzed for (**H**) expression in cell surface and whole cell ELISA as percentage of human $P2Y_{12}$ receptor (non-specific OD value of empty vector was for surface ELISA: 0.06 ± 0.02, whole cell ELISA: 0.04 ± 0.03 each set 0%; and the OD value of $P2Y_{12}$ in surface ELISA: 1.75 ± 0.29; whole cell ELISA: 2.25 ± 0.05, each set 100%) and (**I**) basal and agonistic peptide-stimulated cAMP response shown as x-folds over empty vector (empty vector cAMP levels: 3.8 ± 1.6 nM). Statistics were performed by applying a two-way ANOVA in combination with a Bonferoni post-hoc test: *$p<0.05$; **$p<0.01$; ***$p<0.001$

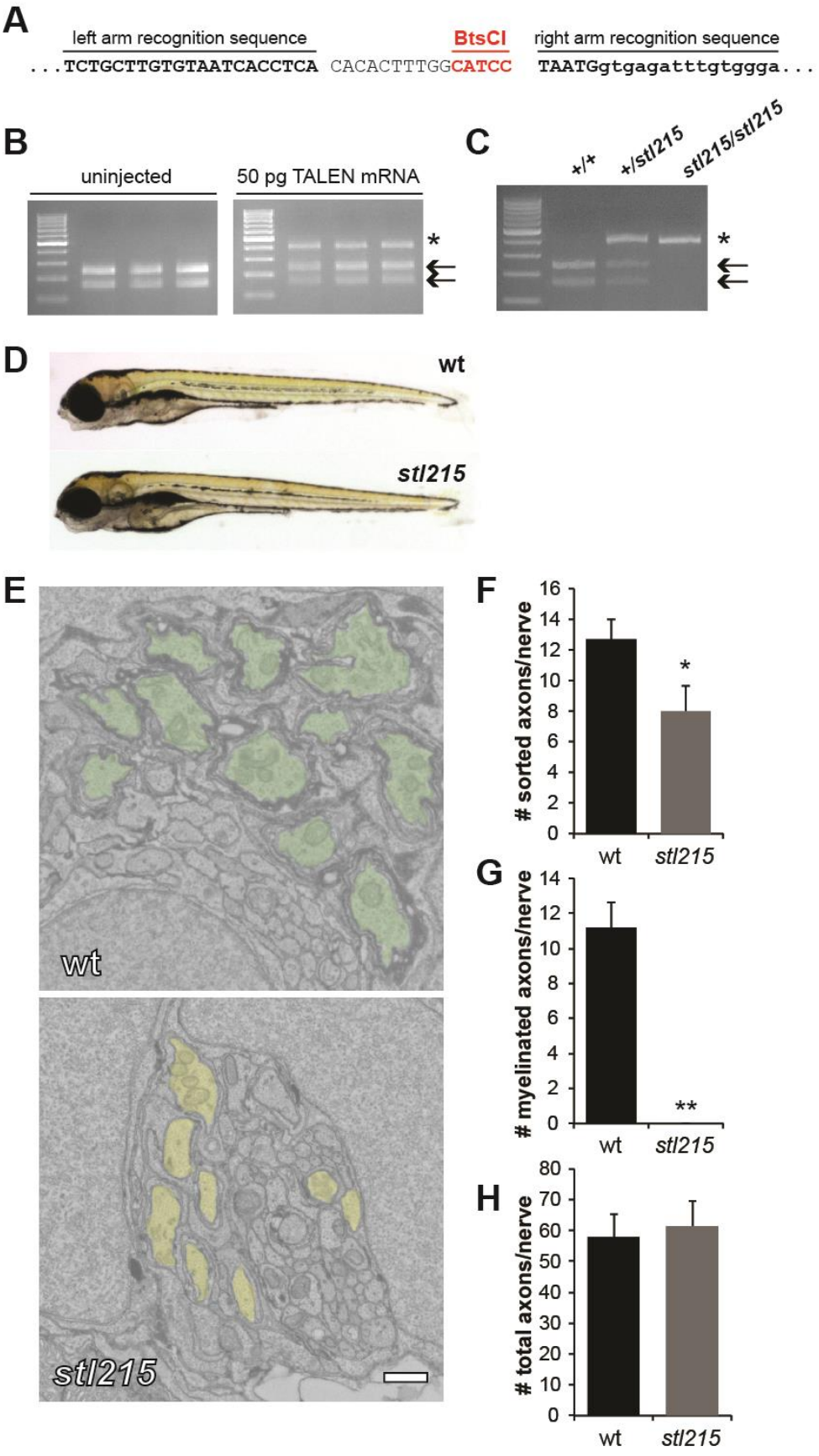
A
left arm recognition sequence
BtsCI
right arm recognition sequence
...TCTGCTTGTGTAATCACCTCA CACACTTTGGCATCC TAATGgtgagatttgtggga...
B
uninjected
50 pg TALEN mRNA
*
C
+/+
+/stl215
stl215/stl215
*
D
wt
stl215
E
wt
stl215
F
sorted axons/nerve
16
14
12
10
8
6
4
2
0
*
wt
stl215
G
myelinated axons/nerve
14
12
10
8
6
4
2
0
**
wt
stl215
H
total axons/nerve
80
70
60
50
40
30
20
10
0
wt
stl215

Suppl. Figure S3. Agonistic peptide deletion ablates Gpr126 function *in vivo*, Related to Figure 4 (**A)** Left and right TALEN recognition sequences in *gpr126*. The unique restriction enzyme site targeted by the TALEN and used for restriction fragment length analysis is underlined in red. Uppercase letters indicate coding sequence, while lowercase letters represent the intronic region. (**B**) Restriction fragment length analysis of three representative uninjected control embryos and three embryos injected with TALEN mRNA (25 pg left arm, 25 pg right arm) at 24 hpf. The arrows mark wild-type fragments cleaved by BtsCI, while the asterisk marks the undigested product resulting from TALEN-mediated disruption of the restriction enzyme site. (**C**) Representative image of the *stl215* genotyping assay using restriction fragment length analysis. The wt PCR product has an intact BtsCI site and the digest results in two fragments of 239 bp and 158 bp (arrows). The disrupted BtsCI site in *stl215* results in an undigested PCR product (asterisk). (**D**) Lateral view of the morphology of a $gpr126^{stl215/+}$ (wt) sibling and a $gpr126^{stl215/stl215}$ mutant at 5 dpf. (**E**) Transmission electron microscopy (TEM) of cross-sections through the PLLn. To control for developmental variability along the anterior-posterior axis, all nerves were analyzed at approximately the same body segment (between segments 5-7) of 5 dpf zebrafish larvae. wt PLLn (top) have many myelinated axons (green), whereas Schwann cells in $gpr126^{stl215}$ sort axons (yellow) but fail to spiral their membranes to form myelin. Scale bar = 500 nm. (**F-H**) Quantification of TEM images from PLLn of wt ($gpr126^{+/+}$ and $gpr126^{stl215/+}$) and $gpr126^{stl215}$ 5dpf larvae. For all, n=6 PLLn from N=4 wt larvae, and n=6 PLLn from N=4 mutant larvae. Error bars indicate standard deviation, significance determined via Student's t-test. (**F**) Average number of sorted axons per PLLn in wt (12.7 ± 1.4) and mutant (8 ± 1.7) larvae. *$p<0.001$. (**G**) Average number of myelinated axons per PLLn in wt (11.1 ± 1.5) and mutant (0 ± 0) larvae. **$p<10^{-8}$. (**H**) Average number of total axons per PLLn in wt (57.8 ± 7.7) and mutant (61.5 ± 8.1) larvae. No significant difference was observed ($p>0.4$).

A

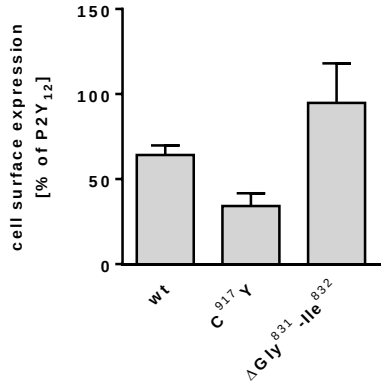

B

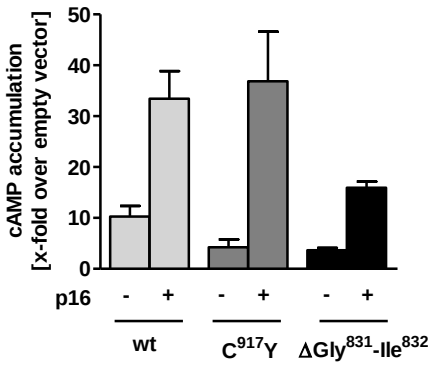

C

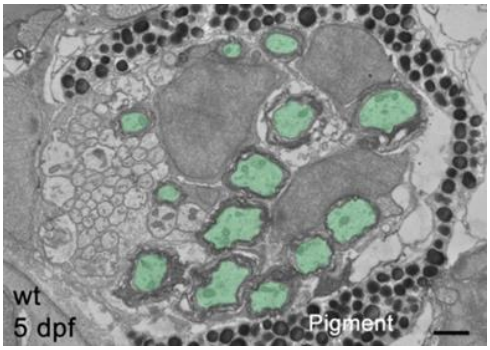

D

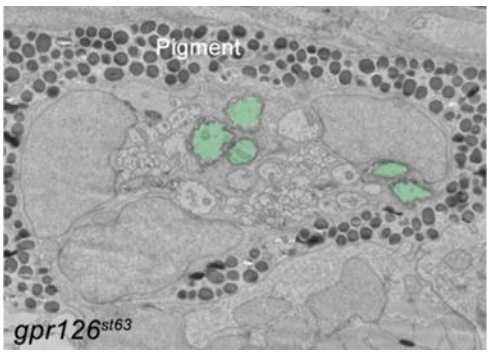

E

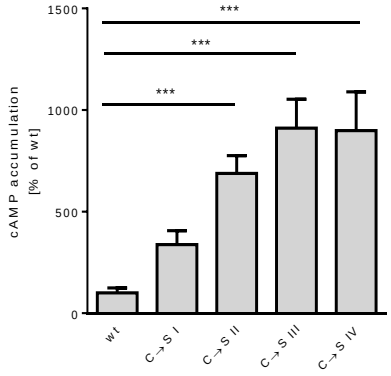

F

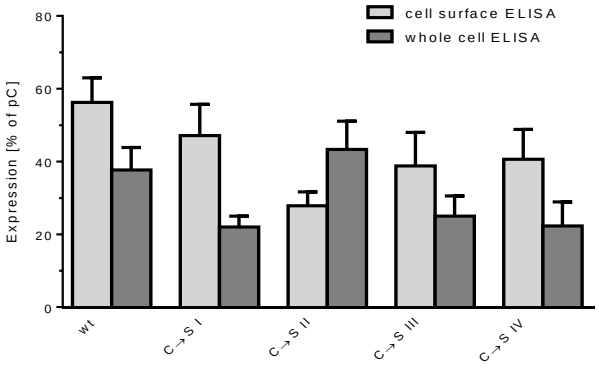

G

```
EMR1    SSFAVLMAHYDVQ
CD97    SSFAILMAHYDVE
GPR56   TYFAVLMVSSVEV
GPR114  TYFAVLMQLSGDP
GPR115  TSFSILMSSKPVK
GPR116  TSFSILMSPDSPD
GPR126  THFGVLMDLPRSA
GPR133  TNFAILMQVVPLE
```

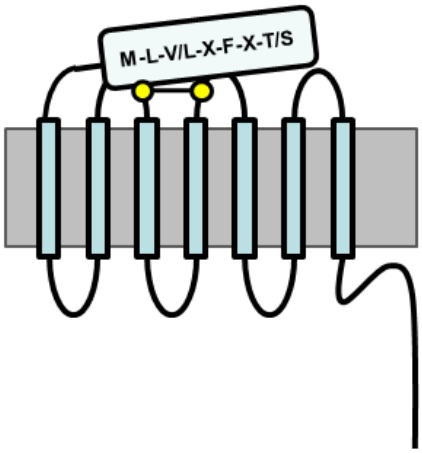

Suppl. Figure S4. Rescue of st63 mutant zebrafish ortholog through p16 and influence of N-terminal positions on GPR126 activity levels, Related to Figure 4

(**A**) COS-7 cells were transiently transfected with wt, $C^{917}Y$ (*gpr126*^{st63}) and ΔGly^{831}-Ile^{832} (*gpr126*^{stl215}) mutant zebrafish Gpr126 constructs and tested for cell surface expression and (**B**) basal and stimulated accumulation of cAMP. For the cell surface ELISA, the non-specific OD value (pcDps) was 0.003 ± 0.001 (set 0%) and the OD value of $P2Y_{12}$ was 1.22 ± 0.33 (set 100%). Data are given as means ± SEM of at least two independent experiments each performed in triplicates. For cAMP assays, empty vector cAMP levels were 1.78 ± 1.12 nM/well. Data are given as means ± SEM of at least two independent experiments performed in triplicates. (**C**-**D**) Transmission electron micrographs (TEM) of 5-day post-fertilization (dpf) larvae showing cross-section through the PLLn. To control for developmental variability along the anterior-posterior axis, all nerves were analyzed at approximately the same body segment (between segments 5-7). (**C**) Myelinated axons are pseudocolored in green in a representative wt larva. (**D**) Myelinated axons are pseudocolored in green in a representative *gpr126*$^{st63/st63}$ mutant larva. For (**C-D**), melanocytes laden with melanin granules are denoted by "pigment". Scale bar = 1 μm. (**E**) To alter GPS structure, disulfide bridge-forming cysteines were systematically mutated to serine in GPR126 ($C^{775}S$/ mutant C→S I, $C^{794}S$/ mutant C→S II, $C^{807}S$/ mutant C→S III and $C^{809}S$/ mutant C→S IV). Interestingly, all mutants displayed constitutive activity in cAMP assay. In all cases, Cys mutations led to a reduction of cell surface expression levels indicating increased intrinsic activity of the mutants. COS-7 cells were transfected with wt and mutant GPR126 constructs. Basal cAMP levels were determined as described under Experimental Procedures. Specific cAMP levels (cAMP value of double HA/FLAG-tagged aGPCR constructs minus cAMP value of mock-transfected cells) were referred to the given wt receptor. Empty vector served as negative control (pcDps; cAMP level: 3.68 ± 2.54 nM/well). For GPR126, basal cAMP levels determined as x-fold over empty vector were 3.70 ± 1.20 (each set 100%). Data are given as means ± SEM of three independent experiments performed in triplicates. Statistics were performed by applying a one-way ANOVA in combination with Bonferoni as post-hoc test: *$p<0.05$; **$p<0.01$; ***$p<0.001$ (**F**) For expression studies, cell surface and whole cell ELISA were used to measure cell surface and total cellular expression levels, respectively. Specific optical density (OD) readings (OD value of double HA/FLAG-tagged aGPCR constructs minus OD value of mock-transfected cells) are given as percentage of the human $P2Y_{12}$ receptor, which served as positive control (pC). For the cell surface ELISA, the non-specific OD value (pcDps) was 0.03 ± 0.03 (set 0%) and the OD value of $P2Y_{12}$ was 1.30 ± 0.24 (set 100%). OD readings of 0.08 ± 0.04 (set 0%) and 2.22 ± 0.73 (set 100%) were found in sandwich ELISA (total expression) for the negative control vector (pcDps) and positive control ($P2Y_{12}$). Data are given as means ± SEM of three independent experiments each performed in triplicates. (**G**) Studies with peptides derived from the first 11-19 amino acid positions downstream the GPS of GPR126 and GPR133 (Figs. 2 and 3) revealed positions in the N terminal half of the *Stachel* sequence that are relevant for its functionality. Many of those positions are highly conserved among aGPCRs. Based on current data, one can speculate that N-terminal cleavage at the GPS, extracellular ligand binding and/or ECD-mediated mechanic signals structurally enable the *Stachel* sequence to function as a peptide agonist for the 7TM.

Suppl. Tab. S1 Description of human GPR126 and human GPR133 constructs used in this study, Related to Figures 1 and 3

construct	deleted amino acid residues	$P2Y_{12}$ amino acid residues	other modifications
GPR133 (wt: 874 aa)	-	-	-
GPR126 (wt: 1222 aa)	-	-	-
GPR126 C→S I	-	-	$C^{775}S$
GPR126 C→S II	-	-	$C^{794}S$
GPR126 C→S III	-	-	$C^{807}S$
GPR126 C→S IV	-	-	$C^{809}S$
GPR126 -CTF	38-812	-	-
GPR133 -CTF	26-544	-	-
GPR126 $P2Y_{12}$ -CTF	1-812	1-34	-
GPR133 $P2Y_{12}$ -CTF	1-544	1-34	-
GPR126 ΔGPS-CTF	38-824	-	-
GPR133 ΔGPS-CTF	26-556	-	-
GPR126 $P2Y_{12}$-ΔGPS-CTF	1-824	1-34	-
GPR133 $P2Y_{12}$-ΔGPS-CTF	1-556	1-34	-
GPR126 CTF -T	38-813	-	-
GPR126 CTF -TH	38-814	-	-
GPR126 CTF -THF	38-815	-	-
GPR126 CTF -THFG	38-816	-	-
GPR126 CTF -THFGV	38-817	-	-
GPR126 CTF -THFGVL	38-818	-	-
GPR126 CTF -THFGVLM	38-819	-	-
GPR126 CTF -THFGVLMD	38-820	-	-
GPR126 CTF -THFGVLMDL	38-821	-	-
GPR126 CTF -THFGVLMDLP	38-822	-	-
GPR126 CTF -$T^{813}A$	38-812	-	$T^{813}A$
GPR126 $P2Y_{12}$- CTF -$T^{813}A$	1-812	1-34	$T^{813}A$
GPR126 CTF -$H^{814}A$	38-812	-	$H^{814}A$
GPR126 $P2Y_{12}$-CTF -$H^{814}A$	1-812	1-34	$H^{814}A$
GPR126 CTF $F^{815}A$	38-812	-	$F^{815}A$
GPR126 $P2Y_{12}$- CTF $F^{815}A$	1-812	1-34	$F^{815}A$
GPR126 CTF $L^{818}A$	38-812	-	$L^{818}A$
GPR126 $P2Y_{12}$-CTF $L^{818}A$	1-812	1-34	$L^{818}A$
GPR126 CTF $M^{819}A$	38-812	-	$M^{819}A$
GPR126 $P2Y_{12}$-CTF-$M^{819}A$	1-812	1-34	$M^{819}A$
GPR126 CTF $P^{822}A$	38-812	-	$P^{822}A$
GPR126 $P2Y_{12}$-CTF $P^{822}A$	1-812	1-34	$P^{822}A$
GPR133 CTF $T^{545}A$	26-544	-	$T^{545}A$
GPR133 $P2Y_{12}$-CTF-$T^{545}A$	1-544	1-34	$T^{545}A$
GPR133 CTF $N^{546}A$	26-544	-	$N^{546}A$

GPR133 $P2Y_{12}$-CTF $N^{546}A$	1-544	1-34	$N^{546}A$
GPR133 CTF $F^{547}A$	26-544	-	$F^{547}A$
GPR133 $P2Y_{12}$-CTF $F^{547}A$	1-544	1-34	$F^{547}A$
GPR133 CTF $L^{550}A$	26-544	-	$L^{550}A$
GPR133 $P2Y_{12}$-CTF $L^{550}A$	1-544	1-34	$L^{550}A$
GPR133 CTF $M^{551}A$	26-544	-	$M^{551}A$
GPR133 $P2Y_{12}$-CTF $M^{551}A$	1-544	1-34	$M^{551}A$
GPR133 CTF $V^{554}A$	26-544	-	$V^{554}A$
GPR133 $P2Y_{12}$-CTF $V^{554}A$	1-544	1-34	$V^{554}A$

Suppl. References

Boselt, I., Rompler, H., Hermsdorf, T., Thor, D., Busch, W., Schulz, A., and Schoneberg, T. (2009). Involvement of the V2 vasopressin receptor in adaptation to limited water supply. PLoS One *4*, e5573.

Czopka, T., and Lyons, D.A. (2011). Dissecting mechanisms of myelinated axon formation using zebrafish. Methods Cell Biol *105*, 25-62.

Gupte, J., Swaminath, G., Danao, J., Tian, H., Li, Y., and Wu, X. (2012). Signaling property study of adhesion G-protein-coupled receptors. FEBS Lett *586*, 1214-1219.

Kimmel, C.B., Ballard, W.W., Kimmel, S.R., Ullmann, B., and Schilling, T.F. (1995). Stages of embryonic development of the zebrafish. Dev Dyn *203*, 253-310.

Liebscher, I., Schoneberg, T., and Promel, S. (2013). Progress in demystification of adhesion G protein-coupled receptors. Biol Chem *394*, 937-950.

Lyons, D.A., Pogoda, H.M., Voas, M.G., Woods, I.G., Diamond, B., Nix, R., Arana, N., Jacobs, J., and Talbot, W.S. (2005). erbb3 and erbb2 are essential for schwann cell migration and myelination in zebrafish. Curr Biol *15*, 513-524.

Moriguchi, T., Haraguchi, K., Ueda, N., Okada, M., Furuya, T., and Akiyama, T. (2004). DREG, a developmentally regulated G protein-coupled receptor containing two conserved proteolytic cleavage sites. Genes Cells *9*, 549-560.

Rompler, H., Yu, H.T., Arnold, A., Orth, A., and Schoneberg, T. (2006). Functional consequences of naturally occurring DRY motif variants in the mammalian chemoattractant receptor GPR33. Genomics *87*, 724-732.

Schoneberg, T., Schulz, A., Biebermann, H., Gruters, A., Grimm, T., Hubschmann, K., Filler, G., Gudermann, T., and Schultz, G. (1998). V2 vasopressin receptor dysfunction in nephrogenic diabetes insipidus caused by different molecular mechanisms. Hum Mutat *12*, 196-205.

Schroder, R., Janssen, N., Schmidt, J., Kebig, A., Merten, N., Hennen, S., Muller, A., Blattermann, S., Mohr-Andra, M., Zahn, S., *et al.* (2010). Deconvolution of complex G protein-coupled receptor signaling in live cells using dynamic mass redistribution measurements. Nat Biotechnol *28*, 943-949.

Thisse, C., Thisse, B., Halpern, M.E., and Postlethwait, J.H. (1994). Goosecoid expression in neurectoderm and mesendoderm is disrupted in zebrafish cyclops gastrulas. Dev Biol *164*, 420-429.